



# A direction-dependent shear strength criterion for rock joints with two new roughness parameters

Liren Ban<sup>1</sup> · Chengzhi Qi<sup>2</sup> · Chunsheng Lu<sup>3</sup>

Received: 23 February 2018 / Accepted: 9 August 2018 / Published online: 22 August 2018  
© Saudi Society for Geosciences 2018

## Abstract

The surface morphology of a rock joint is closely related to its mechanical properties. To reasonably characterize a rock surface, two new roughness parameters were proposed in this paper. One is related to the average slope angle of asperities that contribute to the shear strength, and the other reflects the frictional behavior of asperities that is defined as the maximum possible contact area in the shear direction. Taking the standard joint roughness coefficient profiles as example, these two roughness parameters can be applied to describe the directional characteristics of shear strength. Based on their relationships with initial dilation angles, the proposed roughness parameters were incorporated into a peak shear strength criterion. It is shown that the predicted peak shear strength is consistent with experimental data, and there is a power-law relationship. The application range of new roughness parameters was determined, which may facilitate a measurement process.

**Keywords** Rock joints · Rectangular-shaped asperities · Rock surface morphology · Roughness parameters

## Introduction

Prediction on the shear strength of rock joints is important for safety of rock structures, such as the slope stability, tunnel excavation, durability of dam foundations, and design of rock-socketed piles (Wang et al. 2001; Salari-Rad et al. 2013). It is helpful to a better understanding of the triggering mechanism of earthquakes that mainly occur between faults or plate boundaries due to the stick-slip frictional instability

(Scholz 1998). Shear tests of rock joints in laboratory are usually performed with two methods (Olsson and Barton 2001). One is under a constant normal load with unconstrained normal displacement, and the other is under a constant normal stiffness with constrained normal displacement.

Shear strength of rock joints depends on the mechanical properties of an intact rock, normal stress, surface morphology, and shear direction. Of all these factors, roughness of surface morphology is closely related to the mechanical properties of rock joints. A number of statistical parameters have been proposed to characterize surface roughness, such as the average height ( $Z_0$ ), rms ( $Z_1$ ), the rms of its first derivative ( $Z_2$ ), average roughness angle ( $i_{ave}$ ), structure function, and roughness profile indexes ( $R_p$ ) (Liu et al. 2017). However, these parameters have limitation in establishing connection with the directionality of shear strength of rock joints. Especially, different morphologies might exhibit the same statistical parameters (Huang et al. 1992). Fractal has been applied to characterize the roughness of surface morphology (Xie et al. 1997). The fractal dimension  $D$  may perfectly describe the fine surface such as in the situation of smooth metal friction (Kang et al. 2005); however, it cannot be directly used in evaluating the mechanical properties of rock surfaces with a large-scale size of roughness (Yi et al. 2006). In addition, fractal dimension cannot reflect the directionality of shear strength of rock joints.

---

✉ Chengzhi Qi  
qichengzhi65@126.com

Liren Ban  
18800106123@163.com

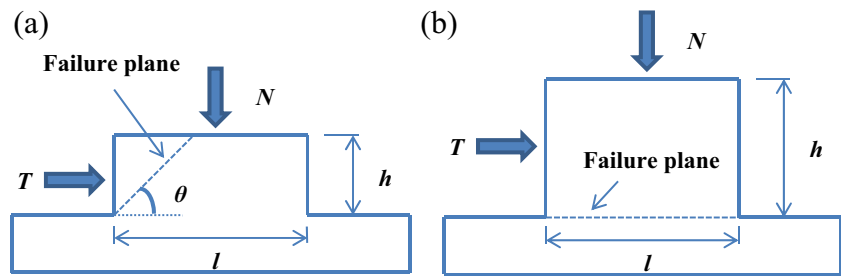
Chunsheng Lu  
C.Lu@curtin.edu.au

<sup>1</sup> School of Mechanics and Civil Engineering, China University of Mining & Technology (Beijing), Beijing 100083, China

<sup>2</sup> Beijing Future Urban Design High-Tech Innovation Center and 2011 Energy Conservation and Emission Reduction Collaborative Innovation Center, Beijing University of Civil Engineering and Architecture, Beijing 100044, China

<sup>3</sup> School of Civil and Mechanical Engineering, Curtin University, Perth, Western Australia 6845, Australia

**Fig. 1** Two shear failure modes of rectangular asperities: **a** dilative failure ( $m < m_c$ ) and **b** non-dilative failure ( $m > m_c$ ), where  $N$  is the normal force and  $T$  is the shear force



Patton (1966) firstly studied the influence of surface morphology on the shear strength of rock joints and obtained a bilinear criterion describing the shear strength of a plane surface with regularly spaced teeth. However, it failed to take into account the variation of peak dilation angles. Maksimović (1992) proposed a criterion to describe the relationship between the peak dilation angle and normal stress. Barton (1973) suggested an equation for estimating the dilation angle  $i = JRC \log_{10}(JCS/\sigma_n)$ , where JRC (joint roughness coefficient) is a parameter that reflects the roughness of rock joints and JCS (joint compressive strength) is the compressive strength of a joint surface. When the joint surface is fresh, JCS is equal to the uniaxial compressive strength of intact rock. Ten standard JRC profiles have been proposed to estimate the roughness of a rock surface through visual comparison, which is subjective and mainly depends on the experience of investigators. Although some limitation remains, JRC was also suggested as a useful index for describing discontinuities. To obtain an objective and quantitative method, the relationship between the statistical parameters and JRC was investigated (Tse and Cruden 1979; Maerz et al. 1990; Lee et al. 1990). However, these approaches are ineffective in getting the JRC value of rock surfaces. The JRC value can be only accurately obtained by back-analysis of shear test results.

However, it is shear strength rather than the JRC value that we want to obtain. The shear strength should be deduced from new roughness parameters with a clear physical meaning.

Experimental results showed that for the same rock type and surface morphology, shear strength changes when the shear direction is different (Jing 1990). Subjected to a shear load, asperities with the slope facing to the shear direction contact and deform, while ones with the slope opposite to the shear direction separate from each other (Yeo et al. 1998; Gentier et al. 1997). The local apparent dip of asperities with respect to the shear direction contributes to the shear strength of rock joints (Grasselli and Egger 2003). Reasonable roughness parameters should reflect the directionality of a rock surface.

In this paper, two new roughness parameters are proposed, providing the possibility to objectively quantify the roughness of rock joints. Moreover, these two roughness parameters can predict the shear strength of rock joints in different directions. To estimate the peak shear strength, a new equation is proposed and further validated by experimental data (Xia et al. 2014).

### The shear behavior of rock asperities

The asperities between joints can be replaced by equivalent rectangular asperities (Kwon et al. 2010). When normal and shear loads are applied, the rectangular asperity exhibits two failure modes: dilative and non-dilative failure, as illustrated in Fig. 1.

The aspect ratio  $m = h/l$ , where  $h$  and  $l$  are the height and length of an asperity, and the critical aspect ratio  $m_c$  jointly determine the failure mode. When  $m$  is less than  $m_c$ , the mode is dilative failure (see Fig. 1a), and the angle between the failure plane and horizontal direction is  $\theta = 45^\circ - \varphi_f/2$ , where  $\varphi_f$  is the peak friction angle of an intact rock. When  $m$  is more

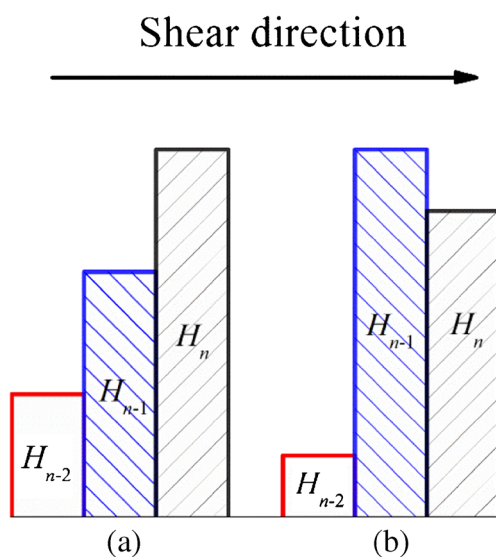


**Fig. 2** The two typical types of rectangular-shaped asperities. The shear direction is from left to right

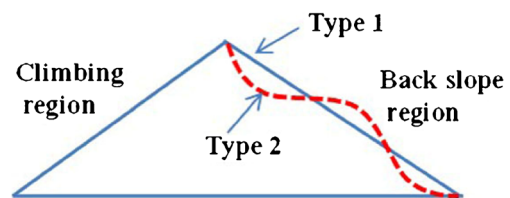
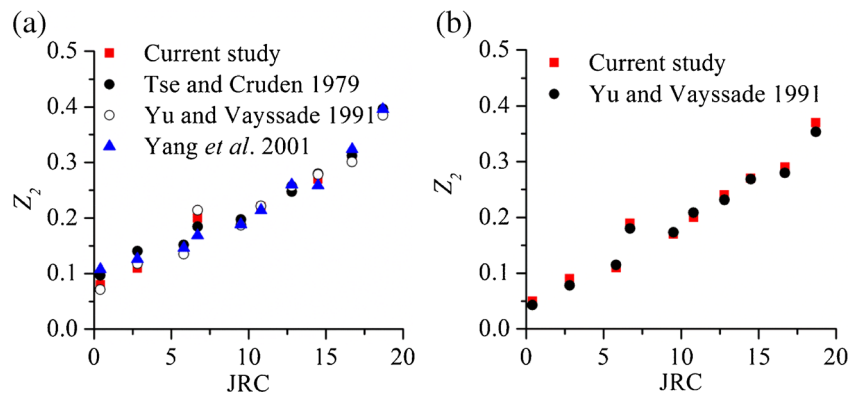


**Fig. 3** Illustration of two types of asperities

**Fig. 4** The value of  $Z_2$  of each standard JRC profile with a sampling interval of **a** 0.5 mm and **b** 1 mm



than  $m_c$ , the mode is non-dilative failure (see Fig. 1b). The failure plane is horizontal and there is no dilation in the whole shear process.

The critical aspect ratio  $m_c$  is obtained as

$$m_c = \frac{c + \sigma_n \tan \varphi_f}{2\tau_c \tan(\varphi_f + 45^\circ) + \sigma_n \tan^2(\varphi_f + 45^\circ)} \quad (1)$$

where  $\sigma_n$  is the normal stress and  $\tau_c$  is the cohesion of an intact rock. The shear strength of a single rectangular asperity is represented by

$$\begin{cases} \tau = 2m\tau_c \tan(\varphi_f + 45^\circ) + m\sigma_n \tan^2(\varphi_f + 45^\circ) & m < m_c \\ \tau = \tau_c + \sigma_n \tan \varphi_f & m > m_c \end{cases} \quad (2)$$

Given that a reasonable model relating the shear behavior of the whole surface with that of a single asperity, the shear strength of rock joints can be determined. However, the rough surface involves reciprocal extrusion, shearing, friction, and gap between asperities; it is difficult to determine the shear strength of a whole joint surface by accurately calculating the shear strength of every single asperity.

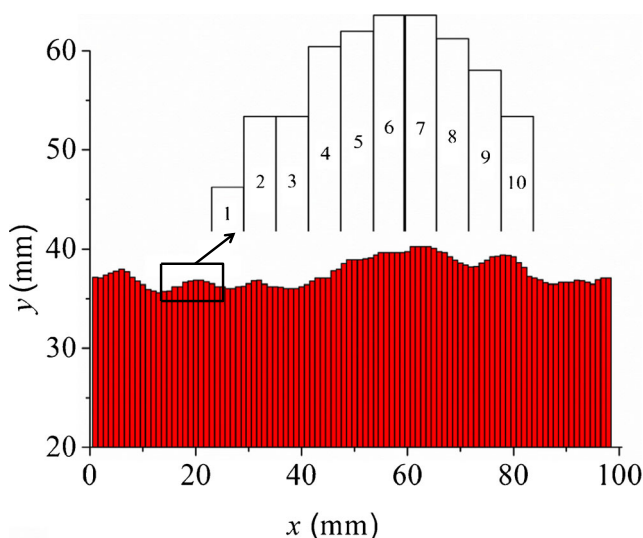


**Fig. 5** The asperities of JRC = 16.7 profile with the sampling interval of 1 mm

As shown in Fig. 2(a), the height of asperities increases along the shear direction. The reduced height of the  $n$ -th asperity can be represented by the height difference, i.e.,  $h_n = H_n - H_{n-1}$ . In Fig. 2(b), the height of the  $n$ -th asperity is less than that of the  $(n-1)$ -th asperity. Because the  $n$ -th asperity is protected by the  $(n-1)$ -th asperity from participating in the interaction between two asperities, the reduced height of the  $n$ -th asperity is 0. However, if the height of the  $(n-2)$ -th asperity is less than that of the  $(n-1)$ -th and  $n$ -th asperities and their protrusions are obvious, it is necessary to consider the influence of the  $(n-2)$ -th asperity. Therefore, the reduced height of the  $n$ -th asperity is taken as an average of  $p$  and  $q$ , where  $p$  is the height difference between the  $n$ -th and  $(n-1)$ -th asperities and  $q$  is the height difference between the  $n$ -th asperity and the  $(n-2)$ -th asperity, and thus,  $h_n = \max[(2H_n - H_{n-1} - H_{n-2})/2, 0]$ . Based on the reduced height of a single asperity, the roughness parameter  $c$  of the entire surface is presented as  $c = 100 \sum_1^N h_n / L$ , where  $L$  is the projection length of a morphology profile and  $N$  is the total number of asperities in the shear direction. Here, it is worth noting that  $c$  is the average slope angle in the shear direction. If the rock surface contains a number of regularly spaced teeth with an equal inclination angle (Patton 1966),  $c$  is equal to  $100 \tan i$ , where  $i$  is the inclination angle of teeth.

### The frictional behavior of rock asperities

The maximum possible contact area reflects the degree of roughness of a rock surface (Grasselli and Egger 2003). The joint surface can be divided into two regions (see Fig. 3). One is the climbing region involving extrusion, wear, and shearing

**Table 1** The value of  $c$  for standard JRC profiles in two different directions

| JRC   | 2.8  | 5.8  | 6.7  | 9.5  | 10.8  | 12.8  | 14.5  | 16.7  | 18.7  |
|-------|------|------|------|------|-------|-------|-------|-------|-------|
| $c_F$ | 3.11 | 4.64 | 7.06 | 7.23 | 9.43  | 11.97 | 13.38 | 13.67 | 16.84 |
| $c_R$ | 3.52 | 7.83 | 9.19 | 5.94 | 11.88 | 12.64 | 16.16 | 13.64 | 18.65 |

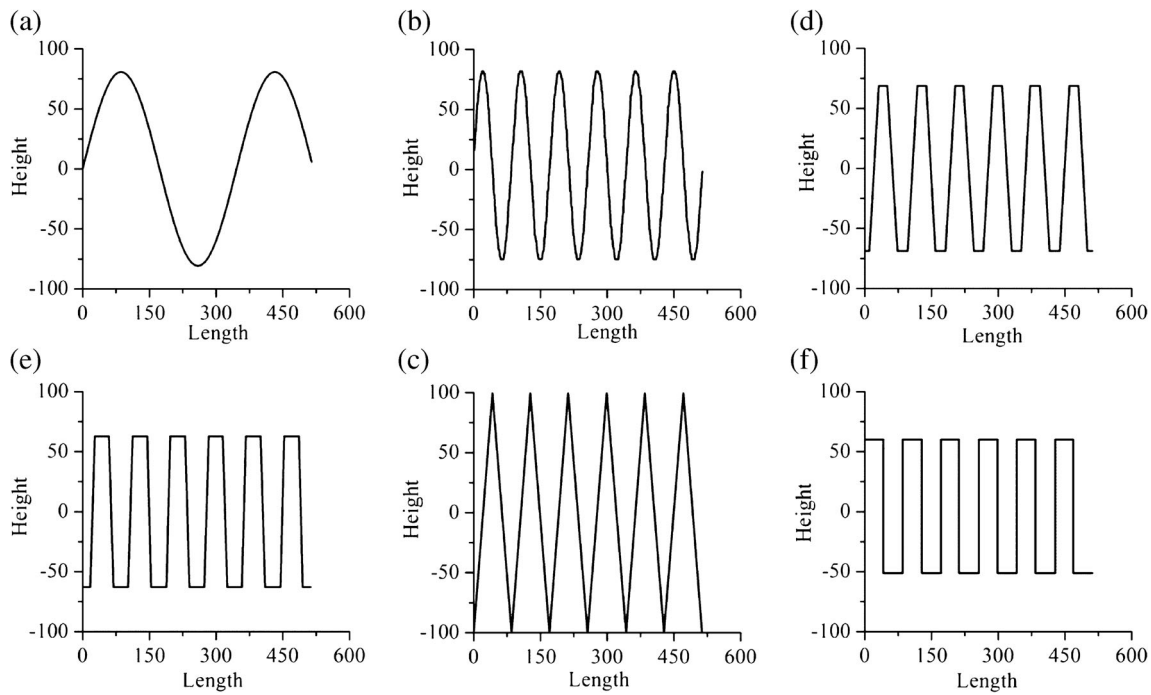


**Fig. 6** A set of profiles with the same  $Z_0$  and  $Z_1$  (Yi et al. 2006), where the value of  $c$  is **a** 7.19, **b** 11.99, **c** 16.79, **d** 21.58, **e** 26.38, and **f** 31.11

between contact asperities, which mainly affects shear strength. The other is the back slope region, which has little effect on shear strength. Therefore, it is necessary to establish a roughness parameter reflecting the friction behavior of the surface morphology according to the climbing region.

Grasselli and Egger (2003) proposed that the maximum possible contact area ratio  $A_0$  is that of  $A_d$  to  $A_t$ , where  $A_d$  is the total climbing area facing to the shear direction and  $A_t$  is the actual area of the joint surface, namely

$$A_0 = \frac{A_d}{A_t} \tag{3}$$

For a three-dimensional grid, we have

$$A_t = (\Delta x \Delta y) \sum_{i=1}^{N_x-1} \sum_{j=1}^{N_y-1} \sqrt{1 + \left(\frac{z_{i+1,j} - z_{i,j}}{\Delta x}\right)^2 + \left(\frac{z_{i,j+1} - z_{i,j}}{\Delta y}\right)^2} \tag{4}$$

where

$N_x$  is the number of points along the  $x$ -axis,  
 $N_y$  is the number of points along the  $y$ -axis,  
 $\Delta x$  and  $\Delta y$  are the sampling steps along  $x$  and  $y$  axes, and

$\Delta x$  and

$\Delta y$

$Z_{ij}$  is the height of the sampling point  $(i, j)$  (Belem et al. 2000).

The maximum possible contact area ratio  $A_0$  reflects the initial characteristics of the surface morphology, with a range of  $0 < A_0 < 1$ . However,  $A_0$  does not take into account the conditions with the same climbing area but different back slope areas.

Because the back slope regions do not affect the shear mechanical properties (see Fig. 3), the shear mechanical properties of the two types of asperities are the same. Here, a reasonable roughness parameter should be identical. However, the roughness parameter  $A_0$  is different, which cannot link with the shear strength. Therefore, the parameter  $A_t$  in Eq. (3) was amended as the nominal area  $A_n$ , which is defined as the projection of the joint surface on its mean plane.

A new roughness parameter  $A_1$  is proposed as

$$A_1 = \frac{A_d}{A_n} \tag{5}$$

with

**Fig. 7** The whole JRC = 6.7 profile and the line segments with an apparent dip angle more than  $0^\circ$

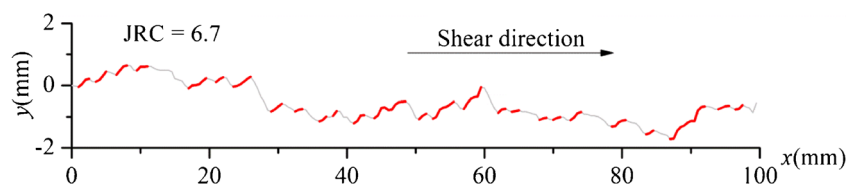


**Table 2** The value of  $A_1$  for standard JRC profiles in two different directions

| JRC      | 2.8  | 5.8  | 6.7  | 9.5  | 10.8 | 12.8 | 14.5 | 16.7 | 18.7 |
|----------|------|------|------|------|------|------|------|------|------|
| $A_{1F}$ | 0.19 | 0.28 | 0.34 | 0.42 | 0.31 | 0.43 | 0.41 | 0.50 | 0.43 |
| $A_{1R}$ | 0.20 | 0.53 | 0.53 | 0.35 | 0.47 | 0.47 | 0.50 | 0.42 | 0.61 |

$$A_n = N_x N_y \Delta x \Delta y \tag{6}$$

where the roughness parameter  $A_1 > 0$  shows the initial characteristics of the surface morphology and stresses the importance of the climbing region.

### Roughness parameters $c$ and $A_1$

#### Acquisition of ten standard JRC profiles

The image segmentation technology was adopted to obtain the coordinate information of the ten standard JRC profiles. With the help of Matlab software, the image information of the JRC profile was transformed into a matrix that stores the gray value of each pile. The pixel whose gray value is smaller than a given threshold was transformed to 0, and such pixels are the points on the standard JRC profile. The coordinates of the JRC profile were obtained after the length of a profile being scaled up to the standard length of 10 cm. In the printing process, due to the problem of typesetting, the profile and the 10-cm scale bar may not be aligned parallel. If the best-fitted line of points lying on each standard profile is not parallel to the scale bar, the corresponding angle should be adjusted. The roughness parameter  $Z_2$  is usually applied to demonstrate the roughness of the surface profiles (Tse and Cruden 1979). Compared with those given by Tse and Cruden (1979), Yu and Vayssade (1991), and Yang et al. (2001), the results obtained are well consistent with the previously published results

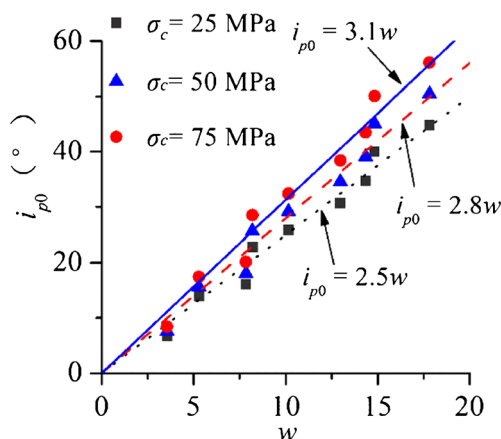


**Fig. 8** The relationship between  $i_{p0}$  and  $w$

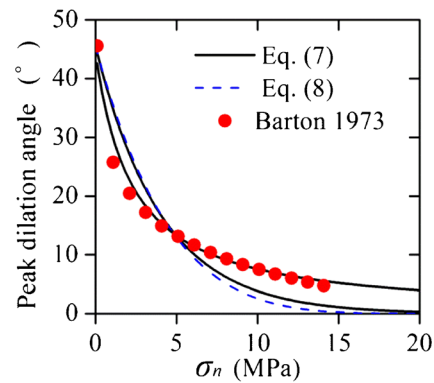


**Fig. 9** Comparison between testing and theoretical results

(Fig. 4), indicating that the extracted data in this method can well reflect the roughness of standard JRC profiles.

#### Calculation of roughness parameter $c$

It is shown that the size of the damaged asperities is on the order of millimeters (Tatone and Grasselli 2010), so the sampling interval was chosen as 1 mm. Then, the coordinate information of the JRC = 16.7 profile was obtained, which is equivalent to continuous rectangular asperities. As shown in Fig. 5, if the local no. 1 asperity is the first asperity of the whole profile, its reduced height is 0. There is only one single asperity in front of no. 2 asperity, and then the reduced height is obtained as  $h_2 = \max[H_2 - H_1, 0]$ . There are two asperities in front of no. 3 asperity, considering the influence of the two front asperities; the reduced height of no. 3 asperity is obtained as  $h_3 = \max[(2H_3 - H_2 - H_1)/2, 0]$ . Similar to no. 3 asperity, the reduced heights of the rest of asperities are all calculated as  $h_n = \max[(2H_n - H_{n-1} - H_{n-2})/2, 0]$ . The parameters  $c$  obtained from the ten standard JRC profiles with the sampling interval of 1 mm are listed in Table 1. The value of JRC was determined through back-analyzing of shear test results on standard JRC profiles (Barton 1973).  $c_F$  and  $c_R$  denote the parameter  $c$  for shearing in forward and reverse direction, respectively. The roughness parameter  $c$  can distinguish the roughness of the same standard JRC profile in different directions, which provides the possibility to propose a new shear strength equation reflecting the direction-dependency of shear strength of rock joints.

The six sets of morphology profiles with horizontal and vertical coordinates being normalized by the same scale in Fig. 6 cannot be distinguished from each other using the roughness parameters of  $Z_0$  and  $Z_1$  (Yi et al. 2006). However, these profiles can be distinguished well with the parameter  $c$ .

#### Calculation of roughness parameter $A_1$

The JRC = 6.7 profile can be approximated by fragments that are formed by linking the adjacent points extracted from the

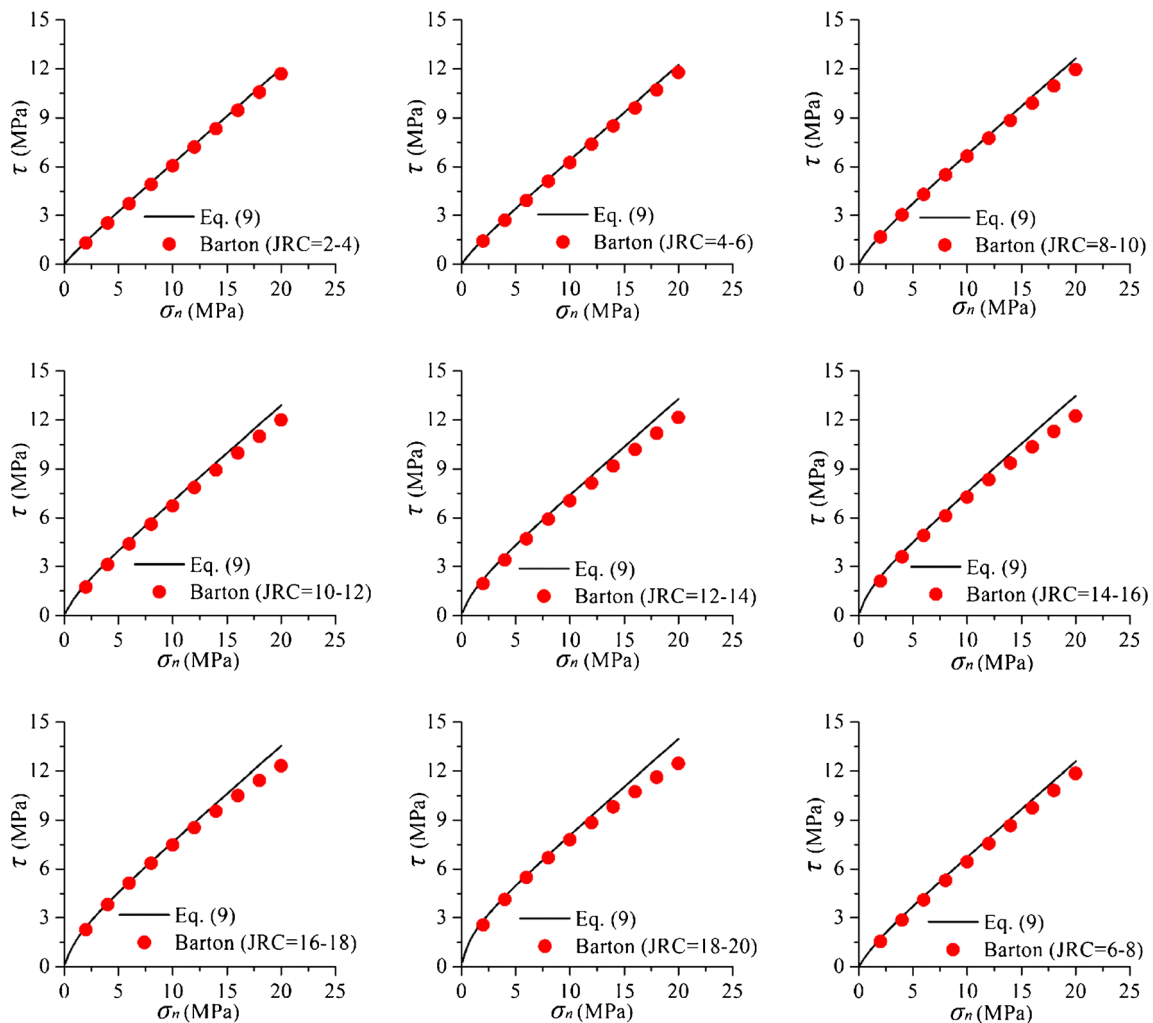


Fig. 10 Comparison of testing results and the calculated values by using Eq. (9) for each standard JRC profile

JRC = 6.7 profile with the sampling interval of 1 mm (see Fig. 7). Based on Eq. (5), the roughness parameter  $A_1$  of JRC = 6.7 profile is the ratio of the length of all the red lines (with dip angle more than  $0^\circ$ ) to the horizontal projection length of the profile. The parameter  $A_1$  of the standard JRC profiles with the sampling interval of 1 mm is listed in Table 2.  $A_{1L}$  and  $A_{1R}$  denote the parameter  $A_1$  for shearing in forward and reverse direction, respectively. Similar to the parameter  $c$ ,

when JRC is the same, the parameter  $A_1$  obtained in different directions is different.

### A new shear strength criterion

According to the Mohr–Coulomb criterion,  $\tau = \sigma_n \tan(\varphi_b + i_p)$ , where  $\varphi_b$  is the basic friction angle and  $i_p$  is the peak dilation angle. The basic friction angle is constant while the peak dilation angle varies with the normal stress. Therefore, the key to study the peak shear strength is how to determine the peak dilation angle reasonably.

The peak shear strength equation proposed by Maksimović (1992) is represented as

$$\tau = \sigma_n \tan \left[ \varphi_b + \frac{\Delta\varphi}{1 + (\sigma_n/p_N)} \right] \tag{7}$$

where  $\Delta\varphi$  is the inclination of the steepest asperities and is equal to the initial dilation angle and  $p_N$  is the median angle pressure when the peak dilation angle is equal to  $\Delta\varphi/2$ . In Eq.

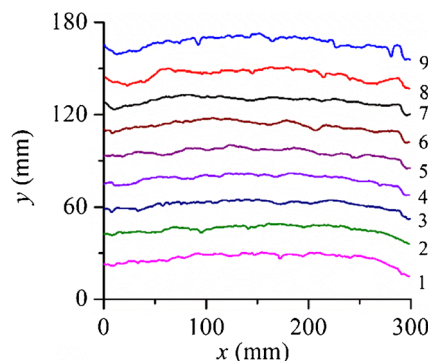


Fig. 11 The map of rock surfaces (Xia et al. 2014)

**Table 3** The value of new roughness parameters of nine profiles (Xia et al. 2014)

| Num.           | 1     | 2     | 3     | 4     | 5     | 6     | 7     | 8     | 9     | Ave.  |
|----------------|-------|-------|-------|-------|-------|-------|-------|-------|-------|-------|
| c              | 13.97 | 10.62 | 11.33 | 10.45 | 9.33  | 11.37 | 9.87  | 15.86 | 21.83 | 12.74 |
| A <sub>1</sub> | 0.45  | 0.44  | 0.43  | 0.42  | 0.39  | 0.45  | 0.45  | 0.48  | 0.54  | 0.45  |
| w              | 15.00 | 11.62 | 12.32 | 11.43 | 10.22 | 12.40 | 10.89 | 16.97 | 23.09 | 13.77 |

(7), there is no singular point when the normal stress is zero; however, it is necessary to get at least three dilation angle-normal stress data points to calculate  $\Delta\varphi$ . Therefore, how to reasonably determine  $\Delta\varphi$  is the key to improve the applicability of Eq. (7).

The initial dilation angle only depends on the roughness of a rock surface (Ghazvinian et al. 2010). The two roughness parameters reflect shear strength and the characteristics of friction, and then, the shearing action can be comprehensively reflected by a parameter,  $w = c + 2.3A_1$ , where 2.3 represents the proportion of friction. The relationship between the roughness parameter  $w$  and the initial dilation angle  $i_{p0}$  is proposed as

$$i_{p0} = 1.49\sigma_c^{0.16}w \tag{8}$$

where  $\sigma_c$  is in the unit of megapascals.

The predicted results of  $i_{p0}$  based on Eq. (8) are compared with the test results in Fig. 8. The data of  $i_{p0}$  are obtained based on Barton’s criterion when  $\sigma_c = 25, 50,$  and  $100$  MPa, and the parameter  $w$  is obtained from the standard JRC profiles. The numbers 2.5, 2.8, and 3.1 stand for  $1.49\sigma_c^{0.16}$  in Eq. (8) when  $\sigma_c = 25, 50,$  and  $100$  MPa.

Combining Eq. (7) with Eq. (8), we can obtain

$$\tau = \sigma_n \tan \left[ \varphi_b + \frac{1.49\sigma_c^{0.16}w}{1 + (\sigma_n/p_N)} \right] \tag{9}$$

where  $p_N$  is 0.1 JCS (Maksimović 1996) and  $\sigma_c$  is in the unit of megapascals. The peak dilation angle is determined by

$$i_p = \frac{1.49\sigma_c^{0.16}w}{1 + (\sigma_n/p_N)} \tag{10}$$

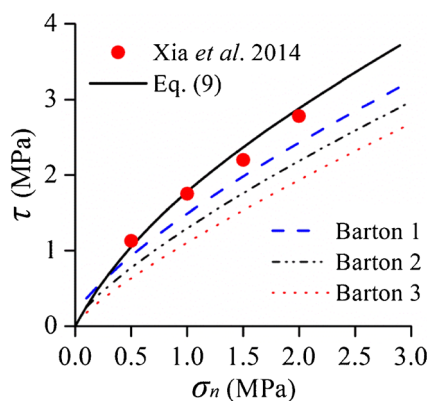


**Fig. 12** Comparison of calculated and testing results (Xia et al. 2014)

According to Schneider (1976) and Jing (1990), the peak dilation angle is individually represented as

$$i_p = i_{p0}e^{-k\sigma_n} \tag{11}$$

and

$$i_p = i_{p0} \left( 1 - \frac{\sigma_n}{\sigma_c} \right)^k \tag{12}$$

For the standard JRC = 10–12 profile, the test and predicted results are compared in Fig. 9, where  $\sigma_c$  is 25 MPa. The coefficients  $k$  in Eqs. (11) and (12) are 0.25 and 5.64, which are obtained by regression analysis. Though the result obtained by Eq. (10) is slightly more than test rest, the trend is better than that fitted by Eqs. (11) and (12).

In Fig. 10, the results based on Eq. (9) are compared with the shear test results of nine standard JRC profiles, where  $\sigma_c = 25$  MPa and the basic friction angle is  $30^\circ$ . For  $JRC < 12$ , Eq. (9) can accurately predict the test results. For  $JRC > 12$ , the results are slightly different from the test results under a high normal stress, but a high degree of coincidence is seen in the range of  $0-0.5\sigma_c$ . This range is also the stress state of most shear tests in engineering (Maksimović 1996).

For the standard JRC profiles, the calculation results of Barton’s equation represent the test results. Inability of accurately determining the JRC values may lead to the lose efficacy of Barton’s equation (Kulatilake et al. 1995; Xia et al. 2014). To further explain the applicability and validity of Eq. (9) for an arbitrary rock surface morphology, the predicted results are compared with the test results (Xia et al. 2014), where the shear direction is from left to right. The surface morphology is represented by nine parallel profiles with an equal distance of 15 mm (see Fig. 11).

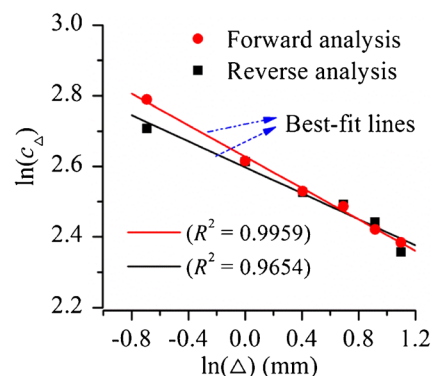


**Fig. 13** The relationship between  $\ln(\Delta)$  and  $\ln(c_\Delta)$

Substituting the average value of  $w$  (see Table 3), the uniaxial compressive strength 27.5 MPa, and the basic friction angle  $35^\circ$  (Xia et al. 2014) into Eq. (9), we can obtain the shear strength. As shown in Fig. 12, Eq. (9) can accurately predict the shear strength of rock joints, where Barton 1 stands for Barton’s equation in which JRC is determined by a straight edge method (Barton and Bandis 1990), Barton 2 stands for Barton’s equation in which JRC is determined by  $Z_2$  (Tse and Cruden 1979), and Barton 3 stands for Barton’s equation in which JRC is determined by visual comparison with the ten standard JRC profiles (Xia et al. 2014). The JRC values obtained by these methods are smaller than the test values.

## Discussion

### The influence of a sampling interval

Natural joint surface has a self-affine fractal character, and its area can be represented as (Xie et al. 1997):

$$A_T(\delta) = A_{T0}\delta^{2-D} \tag{13}$$

where  $A_T(\delta)$  is the area of the rough surface measured by the scale of  $\delta$ ,  $A_{T0}$  is the area measured by the scale of 1 mm, and  $D$  is the fractal dimension of the rough surface. However, the measured surface area with different scales cannot well reflect the shear strength of rock joints, and the fractal dimension  $D$  obtained is independent of the shear direction. Referring to the above method, a power-law relationship is proposed as

$$c_\Delta = c_0\Delta^{1-D_c} \tag{14}$$

where

- $c_\Delta$  is the parameter of  $c$  obtained with the sampling interval of  $\Delta$ ,
- $c_0$  is the parameter of  $c$  obtained with the sampling interval of 1 mm, and
- $D_c$  is the fractal dimension of the morphology profile.

Then, we have

$$D_c = 1 - \frac{\ln\left(\frac{c(\Delta)}{c_0}\right)}{\ln\Delta} \tag{15}$$

The roughness parameters can be obtained with best-fitting lines based on Eq. (15), where the slope is  $1-D_c$ , and the intersection point with vertical coordinate is  $\ln(c_0)$ . When the sampling interval is 0.5, 1, 1.5, 2, 2.5 and 3 mm, the relationship between the parameter  $c_\Delta$  and the sampling interval  $\Delta$  of JRC = 16.7 profile with forward and reverse analysis is shown in Fig. 13. The distribution of  $\ln(c_\Delta)-\ln(\Delta)$  is linear with a relatively high correlation, indicating that the surface

**Table 4** The value of  $D_c$  for each standard JRC profile

| JRC profile | Back-analyzing of shear test results | $D_c$            |                  |
|-------------|--------------------------------------|------------------|------------------|
|             |                                      | Forward analysis | Reverse analysis |
| 0–2         | 0.3                                  | 1.46             | 1.35             |
| 2–4         | 2.8                                  | 1.18             | 1.20             |
| 4–6         | 5.8                                  | 1.35             | 1.33             |
| 6–8         | 6.7                                  | 1.28             | 1.24             |
| 8–10        | 9.5                                  | 1.29             | 1.36             |
| 10–12       | 10.8                                 | 1.10             | 1.15             |
| 12–14       | 12.8                                 | 1.15             | 1.25             |
| 14–16       | 14.5                                 | 1.10             | 1.22             |
| 16–18       | 16.7                                 | 1.22             | 1.18             |
| 18–20       | 18.7                                 | 1.18             | 1.13             |

profile is fractal. The fractal dimensions in forward and reverse directions of each standard JRC profiles are listed in Table 4.

### The range of roughness parameter $c$

The roughness parameter  $c$  of the JRC = 16.7 profile was calculated from the scale of 0.5 to 10 mm with the step of 0.5 mm (see Fig. 14). The data of  $\ln(c_\Delta)-\ln(\Delta)$  has an obvious linear character in the scale range of 0.5–3 mm, in which the profile has a stable fractal dimension. However, the fractal dimension changes greatly when the scale is larger than 3 mm. Yi et al. (2006) also found that the fractal dimension changes with the scale, and when the scale is less than a certain degree, the fractal dimension is stable. The scale of 0.5–3 mm is also the scale of joint failure, and this range can be regarded as the application range of the proposed roughness parameter. In the measurement process, the measurement scale needs not be fixed. The roughness parameter  $c_0$  can be obtained by linear fitting only by knowing two values of  $c$  with two different sampling intervals in this range. This approach reduces the difficulty of obtaining the parameter and is beneficial to a wide application in engineering.

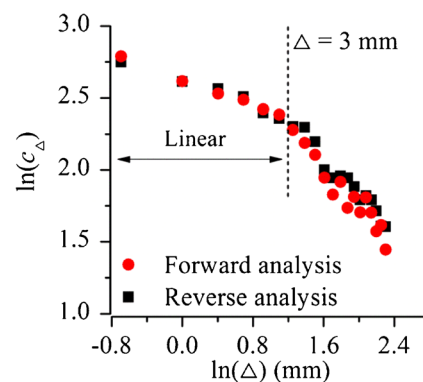


**Fig. 14** The data of  $\ln(c_\Delta)-\ln(\Delta)$  in the range of 0.5 to 10 mm



## Conclusions

In this paper, two roughness parameters of  $c$  and  $A_1$  are proposed. Parameter  $c$  reflects the shear behavior of the rock asperity with the physical meaning being the average slope angle of the rock surface in the direction of shear deformation. Parameter  $A_1$  reflects the frictional behavior of the rock asperity with the physical meaning being the maximum possible contact area in the shear direction. The proposed parameters have advantages in considering surface roughness anisotropy and showing clear mechanical meaning relative to the statistical parameters, and relative to the JRC method, they can be applied to objectively quantify the roughness of rock surface morphology.

The proposed roughness parameters can be incorporated into a new peak shear strength criterion, which are correlated well with the standard JRC shear test results. Furthermore, the predicted values show good agreement with those obtained experimentally. In addition, it is shown that the Mohr–Coulomb criterion is more easily accepted in an engineering point of view. With two different sampling intervals in the sampling interval of 0.5–3 mm, the roughness parameter  $c$  can be obtained by linear fitting. This approach reduces the difficulty of obtaining the new parameter and is beneficial to a wide application in engineering.

**Funding information** This work was supported by the National Key Basic Research Program of China (973) (Project No. 802015CB575) and the National Natural Science Foundation of China (Project Nos. 51478027 and 51774018). C. Lu is supported by the Open Fund of State Key Laboratory for GeoMechanics and Deep Underground Engineering, China University of Mining & Technology (Beijing) (Project No. SKLGDUEK1516).

## References

- Barton N (1973) Review of a new shear-strength criterion for rock joints. *Eng Geol* 7(4):287–332. [https://doi.org/10.1016/0013-7952\(73\)90013-6](https://doi.org/10.1016/0013-7952(73)90013-6)
- Barton N, Bandis S (1990) Review of predictive capabilities of JRC–JCS model in engineering practice. In: *Proceeding of International Conference on Rock Joints*. A, A, Balkema, Rotterdam, pp 603–510
- Belem T, Homand-Etienne F, Souley M (2000) Quantitative parameters for rock joint surface roughness. *Rock Mech Rock Eng* 33(4):217–242 <https://doi.org/10.1007/s006030070001>
- Gentier S, Lamontagne E, Archambault G, Riss J (1997) Anisotropy of flow in a fracture undergoing shear and its relationship to the direction of shearing and injection pressure. *Int J Rock Mech Min Sci* 33(34):412–412. [https://doi.org/10.1016/S0148-9062\(97\)00177-0](https://doi.org/10.1016/S0148-9062(97)00177-0)
- Ghazvinian AH, Taghichian A, Hashemi M (2010) The shear behavior of bedding planes of weakness between two different rock types with high strength difference. *Rock Mech Rock Eng* 43(1):69–87. <https://doi.org/10.1007/s00603-009-0030-8>
- Grasselli G, Egger P (2003) Constitutive law for the shear strength of rock joints based on three-dimensional surface parameters. *Int J Rock Mech Min Sci* 40(1):25–40. [https://doi.org/10.1016/S1365-1609\(02\)00101-6](https://doi.org/10.1016/S1365-1609(02)00101-6)
- Huang SL, Oelfke SM, Speck RC (1992) Applicability of fractal characterization and modelling to rock joint profiles. *Int J Rock Mech Min Sci Geomech Abstr* 29(2):89–98. [https://doi.org/10.1016/0148-9062\(92\)92120-2](https://doi.org/10.1016/0148-9062(92)92120-2)
- Jing L (1990) Numerical modeling of jointed rock masses by distinct element method for two and three dimensional problems. Dissertation, Lulea University of Technology
- Kang MC, Kim JS, Kim KH (2005) Fractal dimension analysis of machined surface depending on coated tool wear. *Surf Coat Technol* 193(1):259–265. <https://doi.org/10.1016/j.surfcoat.2004.07.020>
- Kulatilake PH, Shou G, Huang TH (1995) New peak shear strength criteria for anisotropic rock joints. *Int J Rock Mech Min Sci Geomech Abstr* 32(7):673–697. [https://doi.org/10.1016/0148-9062\(95\)00022-9](https://doi.org/10.1016/0148-9062(95)00022-9)
- Kwon TH, Hong ES, Cho GC (2010) Shear behavior of rectangular-shaped asperities in rock joints. *KSCE J Civ Eng* 14(3):323–332. <https://doi.org/10.1007/s12205-010-0323-1>
- Lee YH, Carr JR, Barr DJ (1990) The fractal dimension as a measure of the roughness of rock discontinuity profiles. *Int J Rock Mech Min Sci Geomech Abstr* 27(6):453–464. [https://doi.org/10.1016/0148-9062\(90\)90998-H](https://doi.org/10.1016/0148-9062(90)90998-H)
- Liu XG, Zhu WC, Yu QL (2017) Estimation of the joint roughness coefficient of rock joints by consideration of two-order asperity and its application in double-joint shear tests. *Eng Geol* 220:243–255. <https://doi.org/10.1016/j.enggeo.2017.02.012>
- Maerz NH, Franklin JA, Bennett CP (1990) Joint roughness measurement using shadow profilometry. *Int J Rock Mech Min Sci Geomech Abstr* 27(5):329–343. [https://doi.org/10.1016/0148-9062\(90\)92708-M](https://doi.org/10.1016/0148-9062(90)92708-M)
- Maksimović M (1992) New description of the shear strength for rock joints. *Rock Mech Rock Eng* 25(4):275–284. <https://doi.org/10.1007/BF01041808>
- Maksimović M (1996) The shear strength components of a rough rock joint. *Int J Rock Mech Mining Sci Geomech Abstr* 33(8):769–783. [https://doi.org/10.1016/0148-9062\(95\)00005-4](https://doi.org/10.1016/0148-9062(95)00005-4)
- Olsson R, Barton N (2001) An improved model for hydromechanical coupling during shearing of rock joints. *Int J Rock Mech Min Sci* 38(3):317–329. [https://doi.org/10.1016/S1365-1609\(00\)00079-4](https://doi.org/10.1016/S1365-1609(00)00079-4)
- Patton F D (1966) Multiple modes of shear failure in rock. *Proceedings of the 1st international congress on rock mechanics*. Lisbon, pp 509–513
- Salari-Rad H, Mohitazar M, Dizadji MR (2013) Distinct element simulation of ultimate bearing capacity in jointed rock foundations. *Arab J Geosci* 6(11):4427–4434. <https://doi.org/10.1007/s12517-012-0667-6>
- Schneider HJ (1976) The friction and deformation behaviour of rock joints. *Rock Mech* 8(3):169–184. <https://doi.org/10.1007/BF01239813>
- Scholz CH (1998) Earthquakes and friction laws. *Nature* 391(6662):37–42. <https://doi.org/10.1038/34097>
- Tatone BSA, Grasselli G (2010) A new 2D discontinuity roughness parameter and its correlation with JRC. *Int J Rock Mech Min Sci* 47(8):1391–1400. <https://doi.org/10.1016/j.ijrmm.2010.06.006>
- Tse R, Cruden DM (1979) Estimating joint roughness coefficients. *Int J Rock Mech Min Sci Geomech Abstr* 16(5):303–307. [https://doi.org/10.1016/0148-9062\(79\)90241-9](https://doi.org/10.1016/0148-9062(79)90241-9)
- Wang WL, Wang TT, Su JJ (2001) Assessment of damage in mountain tunnels due to the Taiwan Chi-Chi Earthquake. *Tunnelling & Underground Space Technology Incorporating Trenchless Technology Research* 16(3):133–150. [https://doi.org/10.1016/S0886-7798\(01\)00047-5](https://doi.org/10.1016/S0886-7798(01)00047-5)
- Xia CC, Tang ZC, Xiao WM (2014) New peak shear strength criterion of rock joints based on quantified surface description. *Rock Mech Rock Eng* 47(2):387–400. <https://doi.org/10.1007/s00603-013-0395-6>
- Xie H, Wang JA, Xie WH (1997) Fractal effects of surface roughness on the mechanical behavior of rock joints. *Chaos, Solitons Fractals* 8(2):221–252. [https://doi.org/10.1016/S0960-0779\(96\)00050-1](https://doi.org/10.1016/S0960-0779(96)00050-1)

- Yang ZY, Lo SC, Di CC (2001) Reassessing the joint roughness coefficient (JRC) estimation using  $Z_2$ . *Rock Mech Rock Eng* 34(3):243–251. <https://doi.org/10.1007/s006030170012>
- Yeo IW, Freitas MD, Zimmerman RW (1998) Effect of shear displacement on the aperture and permeability of a rock fracture. *International Journal of Rock Mechanics & Mining Science* 35(8): 1051–1070. [https://doi.org/10.1016/S0148-9062\(98\)00165-X](https://doi.org/10.1016/S0148-9062(98)00165-X)
- Yi C, Wang CJ, Zhang L (2006) Study on description index system of rough surface based on bi-body interaction. *Chin J Rock Mech Eng* 25(12):2481–2492. <https://doi.org/10.3321/j.issn:1000-6915.2006.12.014>
- Yu X, Vayssade B (1991) Joint profiles and their roughness parameters. *Int J Rock Mech Min Sci Geomech Abstr* 28(4):333–336. [https://doi.org/10.1016/0148-9062\(91\)90598-G](https://doi.org/10.1016/0148-9062(91)90598-G)